Changes in MOC and gyre-induced Atlantic Ocean heat transport

S. S. Drijfhout[1] and W. Hazeleger[1]

Received 19 January 2006; revised 10 February 2006; accepted 15 February 2006; published 4 April 2006.

[1] Anthropogenic change of the Atlantic meridional ocean heat transport (AOHT) is diagnosed from a large ensemble of climate simulations over the period 1940–2080, as well as its relation to changes in the Meridional Overturning Circulation (MOC) and the gyre circulation in the Atlantic. Internal variability in AOHT is closely associated with MOC variability. The anthropogenic change in AOHT, however, does not follow the forced decrease in the MOC. Thermohaline changes in the intermediate and deep water masses that are formed in the subpolar gyre cause the vertical temperature gradient near the western boundary to increase. As a result, the heat transport by the baroclinic gyre component largely compensates the decreased heat transport by the MOC. **Citation:** Drijfhout, S. S., and W. Hazeleger (2006), Changes in MOC and gyre-induced Atlantic Ocean heat transport, *Geophys. Res. Lett.*, *33*, L07707, doi:10.1029/2006GL025807.

1. Introduction

[2] The planetary system receives energy in the form of radiation at the top of the atmosphere. Part of the surplus that is received in the tropics is transported by the atmosphere and ocean to the poles where the energy is lost by longwave radiation. Although the ocean probably carries as little as 10% of the net poleward heat transport at mid-latitudes, removing this heat transport corresponds to an atmospheric radiative forcing change of about 9 W/m^2, larger than what is expected from doubled atmospheric CO_2 [*Wunsch*, 2005]. Typical natural variations in ocean heat transport are one order of magnitude smaller, but still imply a significant forcing term in the planetary heat budget.

[3] North of 30°N, the Atlantic MOC dominates global OHT [*Ganachaud and Wunsch*, 2003]. Most of the variability in AOHT, at least on decadal timescales, is therefore associated with variability of the MOC [*Häkkinen*, 1999; *Dong and Sutton*, 2001; *Eden and Jung*, 2001], which in turn seems to be driven by longer-timescale fluctuations of the NAO [*Dong and Sutton*, 2001; *Eden and Willebrand*, 2001]. On interannual timescales Ekman transport variations dominate. They affect the MOC as well as the wind-driven subtropical cells [*Shaffrey and Sutton*, 2004].

[4] In the extratropics, AOHT and atmospheric heat transport are anticorrelated [*Bjerknes*, 1964]. The anticorrelation becomes stronger when the timescale increases [*Shaffrey and Sutton*, 2006]. In the tropics, heat transport variations in ocean and atmosphere are correlated on interannual timescales as envisaged by the model of *Held* [2001]. Variations in the tropical western boundary current and gyre circulation, however, play a role that was not accounted for [*Hazeleger et al.*, 2004; *Shaffrey and Sutton*, 2004].

[5] In the present study, we investigate whether the decrease of the MOC, which occurs in response to global warming in a large number of models [*Dixon et al.*, 1999; *Mikolajewicz and Voss*, 2000; *Gregory et al.*, 2005], is associated with a similar decrease in AOHT. The analysis of *Hazeleger* [2005] revealed that in some climate models AOHT decreases as a result of a decrease of the MOC; in other models the response of AOHT is weak, suggesting some compensation mechanism for a decrease in MOC-induced heat transport. In the following, we address this question by analyzing a large (62) ensemble of climate model simulations, all forced with increasing levels of greenhouse gas (GHG) concentrations in the atmosphere.

2. Ensemble Experiment

[6] The model used for this study is version 1.4 of the Community Climate System Model (CCSM) of the National Center for Atmospheric Research. The simulations cover the period 1940–2080. Until 2000, the forcing includes specified estimates of temporally evolving solar radiation, temporally and geographically dependent aerosols due to manmade and natural emissions and time dependent GHGs. From 2000 onward all forcings are kept at the 2000 values, except for the concentration of GHGs which increase according to a 'business-as-usual' scenario. For more details on the model and on the ensemble experiment we refer to *Boville et al.* [2001] and *Selten et al.* [2004] respectively.

[7] An ensemble of 62 simulations was produced. The simulations differ only in a small random perturbation to the initial atmospheric temperature field, which leads to completely different weather patterns by the end of the first month. After a few years of spin-up, the ocean circulation in each ensemble member has become decoupled from its initial state. Averaging over all ensemble members filters out most of the internally generated climate variations and allows for an estimate of the externally forced climate signal. Also, by analyzing the detrended timeseries of all ensemble members the internal variability can be much more adequately described than is possible for a single climate-scenario run.

3. Heat Transport and MOC Change

[8] Figure 1a shows the ensemble and time-averaged AOHT over the period 1990–2010. The curve compares well with the estimates derived from atmospheric reanalysis data from *Trenberth and Caron* [2001] and values published by *Ganachaud and Wunsch* [2003]: 0.65 Petawatt (PW) at 30°S is somewhat on the high side (compared to 0.3–

[1]Royal Netherlands Meteorological Institute, De Bilt, Netherlands.

Copyright 2006 by the American Geophysical Union.
0094-8276/06/2006GL025807$05.00

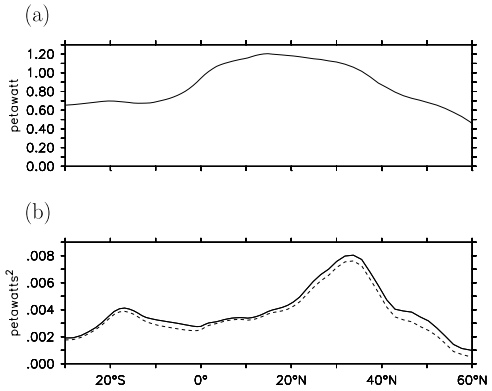

Figure 1. (a) EM and time mean AOHT for the period 1990–2010. (b) Variance of detrended AOHT (solid), together with the amount of variance that is associated with internal MOC-variations (dashes).

0.6 PW); the peak value of 1.20 PW at 15°N is slightly less than the *Ganachaud and Wunsch* [2003] estimate (1.27 PW); 0.45 PW at 60°N is again rather high (0.2–0.3 PW). This heat transport is in accordance with a too strong MOC (a peak value of 30 Sverdrup (Sv) at 40°N and 23 Sv outflow at 30°S) and too weak wind-driven gyres, especially too weak western boundary currents due to a rather coarse resolution of 3.6° in longitude and, outside the tropics, 1.8° in latitude.

[9] Figure 1b shows the variance of AOHT with respect to the ensemble-mean (EM) trend. This represents the internal variability of AOHT. There is a peak around 35°N, well north of the latitude where AOHT is largest, but close to the latitude where the Gulf Stream leaves the American coast. Figure 1b also shows the amount of internal AOHT-variability that is associated with internal MOC-variability. This quantity has been computed by regressing at each latitude the detrended MOC-variability, as determined by the first 100 Empirical Orthogonal Functions which together explain more than 97% of the total amount of internal MOC-variations, on the timeseries of detrended AOHT. At most latitudes the amount of AOHT-variability that can be associated with MOC-variability is about 90%; the ratio between the values of the two curves. Only north of 40°N this amount gradually drops until it becomes 50% at 60°N, but here the total amount of AOHT-variability is very small.

[10] The anthropogenic change in AOHT can be estimated from the linear trend in the EM AOHT at each latitude (Figure 2a). AOHT features negative trends up to 10°N, no change between 10°N and 40°N, and a rise at higher latitudes. Especially the response in the latitude-band between 10°N and 40°N, where AOHT remains almost constant over time, is remarkable. It either suggests a rather complicated response of the MOC to increased greenhouse forcing, or a weak relation between the EM trends in MOC and AOHT, while on the other hand the relation between detrended MOC and AOHT-variance is very tight (Figure 1b). The linear trend in EM MOC (at 1000 m depth where the MOC peaks) is shown in Figure 2b. South of 55°N, the MOC decreases almost uniformly by about 3 Sv per century; north of 55°N the MOC increase is associated with a small overturning cell that results from a shift of the deep water formation site in the Norwegian Sea.

[11] The uniform decrease in the MOC, together with a strong latitudinal dependency of the AOHT-change, implies that the trends in EM MOC and AOHT are unrelated in a large part of the Atlantic. In other words: the relation between MOC-changes and AOHT-changes strongly depends on the time-scale. The regression slope for detrended, unfiltered AOHT-variability on MOC-variability is 0.05 PW/Sv nearly everywhere south of 40°N. When a low-pass filter is applied (20-yr) the regression decreases to 0.04 PW/Sv. The regression slope of the timeseries of EM AOHT on the timeseries of EM MOC is only 0.02 PW/Sv at 30°S, gradually decreasing to 0.01 PW/Sv between 30°N and 50°N. So, the regression of EM AOHT on MOC is a factor of 2.5 smaller than the gain for year-to-year variations at 30°N and decreases further to a factor of 5 smaller at 50°N. We will show in the next section that this is partially due to a compensation of the heat flux associated with the EM MOC by an opposing trend in a separate component associated with the horizontal gyre circulation.

4. Changes in the Gyre Circulation

[12] The poleward heat transport by the gyre is negative everywhere south of 40°N, but much smaller than the poleward heat transport by the overturning circulation. The ensemble mean change in heat transport by the overturning and gyre circulations are comparable, however, but of opposite sign (Figure 3a). The pattern that is associated with the trend (decrease) in the ensemble mean MOC is a single meridional cell that extends over the full latitudinal range of the basin. On the other hand, the response of the gyre circulation to increased GHGs is complicated. It cannot be simply related to a decrease or increase of the gyre as a whole.

[13] To understand how the change in heat transport by the gyre is accomplished, we decompose the advective, time mean part in its various components [*Bryden and Hall*, 1980; *Fanning and Weaver*, 1997]:

$$\overline{[VT]} = \overline{[V'][T']} + \overline{[V^{\star}T^{\star}]} + \overline{[V^{\star}T^{\star}]} \qquad (1)$$

where the overline and square brackets define vertical and zonal averages respectively; the stars and primes define

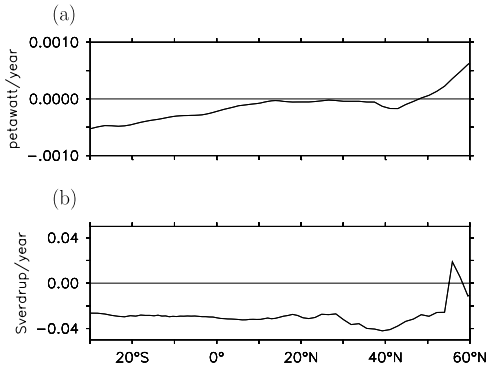

Figure 2. (a) Linear trend in EM AOHT in PW per year. (b) Linear trend in EM MOC at 1000 m depth in Sv per year.

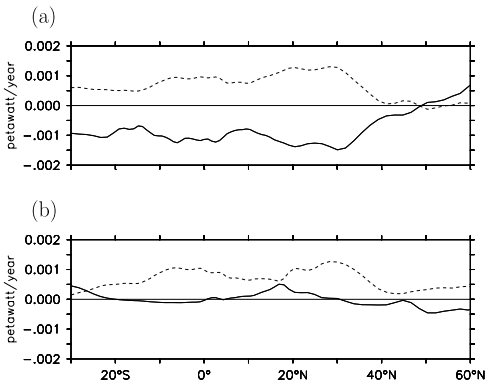

Figure 3. (a) Linear trend in EM AOHT by the overturning component (solid) and gyre component (dashes). (b) Linear trend in EM AOHT by the barotropic gyre component (solid) and baroclinic gyre component (dashes). The individual components are defined in equation (1).

deviations from the zonal and vertical means. The terms at the righthand side can be identified as the overturning, barotropic gyre and baroclinic gyre components. The contributions of the gyre components to the change in EM AOHT are shown in Figure 3b. The baroclinic gyre component clearly dominates the EM trend. It can be interpreted as the heat transport by a stack of closed horizontal, counterrotating circulations that have no net barotropic component. In the Atlantic this circulation manifests itself by a partly overlapping Western Boundary Current (WBC) and Deep (D)WBC, and an interior geostrophic return flow that changes sign with depth.

[14] Figure 4 shows the horizontal pattern of EM change in heat transport by the baroclinic gyre component. The change is almost completely restricted to the western boundary. When the change is decomposed into a part that is due to transport changes and another part that is due to changes in temperature, it is found that the change in heat transport is almost completely due to temperature changes.

[15] Figure 5 shows the EM change in heat transport by the baroclinic gyre, integrated between 77.4°W and 66.6°W which corresponds to the maximum heat transport change displayed in Figure 4. This pattern is overlaid by contours of the baroclinic transport in Sv per layer of 100 *m* depth, integrated over the same longitude-band. We observe increased northward heat transport between 500 and 1000 *m* where the transport is northward and the temperature of watermasses has increased and also between 1500 and 2000 *m* where the transport is southward and the temperature has decreased. The latter contribution is associated with a decrease of Labrador-Irminger Sea Water formation that is apparent in the EM trend in surface heat fluxes. In response to increased GHGs, convection in the western part of the subpolar gyre decreases more rapidly than its eastern counterpart. This result was also obtained by *Wood et al.* [1999].

[16] But the maximum change in EM heat transport by the baroclinic gyre occurs between 3000 and 4000 *m* depth. It is associated with substantial cooling due to increased deep water formation in the Norwegian Sea and a shift in its source region towards cooler waters. The increased deep water formation in the Norwegian Sea partly compensates the decrease of the MOC associated with the decrease of Labrador-Irminger Sea Water formation. Although the increase in deep water formation in the Norwegian Sea is smaller than the decrease in the west, its impact on changes in watermass characteristics and heat transport is much larger. The core of anomalous cold water from the Norwegian Sea is advected cyclonically from the tip of Greenland to the American coast, reaching the western boundary of the Atlantic near 30°N after a few decades and changing the watermasses of the DWBC. Also in response to a decreased MOC, the WBC transports less waters from the Southern Ocean to the northern North Atlantic, which results in heating of the thermocline waters. These changes in vertical temperature gradient near the western boundary are illustrated by Figure 6.

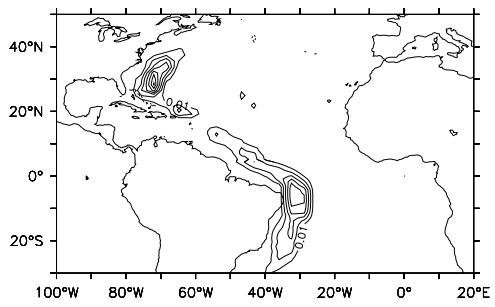

Figure 4. Horizontal pattern of EM change in vertically integrated heat transport by the baroclinic gyre component across a grid boxes of 3.6° width, in Petawatt per century.

5. Discussion and Conclusions

[17] We have shown that, in an ensemble of greenhouse scenario runs, the trends in EM AOHT, MOC and gyre circulation are quite different: increased GHG forcing leads to a reduced MOC, and EM AOHT associated with the MOC decreases as well. Net changes in AOHT, however, are very weak at subtropical latitudes, due to an opposing change in heat transport by the baroclinic gyre. Apparently, increased GHGs force a change in ocean heat content;

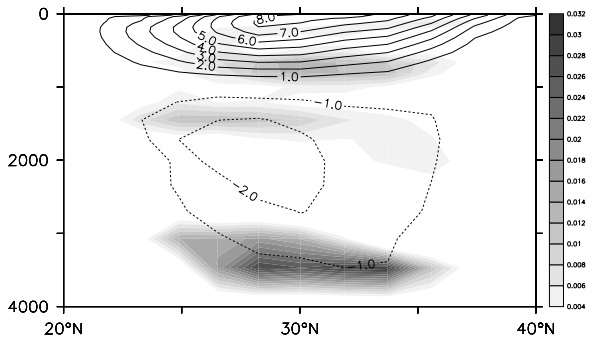

Figure 5. Vertical pattern of EM change in zonally integrated heat transport by the baroclinic gyre component, in Petawatt per century. The zonal integration is between 77.4°W and 66.6°W. This pattern is overlaid by contours of time averaged (full integration period) baroclinic transport in Sv per layer of 100 m depth, integrated over the same longitude-band.

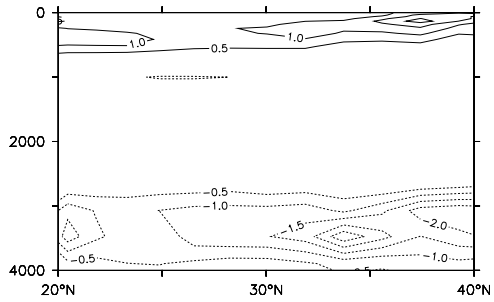

Figure 6. Vertical pattern of EM temperature change in Kelvin per century for the area shown in Figure 5.

especially an increase of the vertical temperature gradient in the region where the WBC and DWBC overlap. On shorter timescales such changes in heat content are negligible. As a result, the internal variability of AOHT is very well correlated with the internal variability of the MOC.

[18] The change in thermohaline water mass properties that is associated with the EM trend, colder intermediate and deep waters in the subpolar North Atlantic, have also been reported by *Joyce et al.* [1999] and *Dickson et al.* [2002]. It appears that, although the model may be unable to simulate the exact details of convection and water mass formation in the North Atlantic, the overall response of the North Atlantic to increased GHGs is rather robust and supported by other models [*Wood et al.*, 1999] and recent observations.

[19] **Acknowledgments.** Computer resources were funded by the National Computing Facilities Foundation (NCF). We thank Michael Kliphuis for technical support, Frank Selten for discussions and two anonymous reviewers who provided insightful comments.

References

Bjerknes, J. (1964), Atlantic air-sea interaction, in *Advances in Geophysics*, vol. 10, pp. 1–82, Elsevier, New York.

Boville, B. A., J. T. Kiehl, P. J. Rasch, and F. O. Bryan (2001), Improvements to the NCAR CSM-1 for transient climate simulations, *J. Clim.*, *14*, 164–179.

Bryden, H. L., and M. M. Hall (1980), Heat transport by currents across 25°N latitude in the Atlantic Ocean, *Science*, *207*, 884–886.

Dickson, B., I. Yashayaev, J. Meincke, B. Turrell, S. Dye, and J. Holfort (2002), Rapid freshening of the deep North Atlantic over the past four decades, *Nature*, *416*, 832–836.

Dixon, K., T. Delworth, M. Spelman, and R. Stouffer (1999), The influence of transient surface fluxes on North Atlantic overturning in a coupled GCM climate change experiment, *Geophys. Res. Lett.*, *26*, 2749–2752.

Dong, B. W., and R. T. Sutton (2001), The dominant mechanisms of variability in Atlantic Ocean heat transport in a coupled GCM, *Geophys. Res. Lett.*, *28*, 2245–2448.

Eden, C., and T. Jung (2001), North Atlantic interdecadal variability: Oceanic response to the North Atlantic Oscillation (1865–1997), *J. Clim.*, *14*, 676–691.

Eden, C., and J. Willebrand (2001), Mechanism of interannual to decadal variability of the North Atlantic circulation, *J. Clim.*, *14*, 2266–2280.

Fanning, A. F., and A. J. Weaver (1997), A horizontal resolution and parameter sensitivity study of heat transport in an idealized coupled climate model, *J. Clim.*, *10*, 2469–2478.

Ganachaud, A., and C. Wunsch (2003), Large-scale ocean heat and freshwater transports during the World Ocean Circulation Experiment, *J. Clim.*, *16*, 696–705.

Gregory, J. M., et al. (2005), A model intercomparison of changes in the Atlantic thermohaline circulation in response to increasing atmospheric CO_2 concentration, *Geophys. Res. Lett.*, *32*, L12703, doi:10.1029/2005GL023209.

Häkkinen, S. (1999), Variability of the simulated meridional heat transport in the North Atlantic for the period 1951–1993, *J. Geophys. Res.*, *104*, 10,991–11,007.

Hazeleger, W. (2005), Can global warming affect tropical ocean heat transport?, *Geophys. Res. Lett.*, *32*, L22701, doi:10.1029/2005GL023450.

Hazeleger, W., R. Seager, M. Cane, and N. Naik (2004), How can tropical Pacific ocean heat transport vary?, *J. Phys. Oceanogr.*, *34*, 1967–1983.

Held, I. M. (2001), The partitioning of the poleward energy transport between the tropical ocean and atmosphere, *J. Atmos. Sci.*, *58*, 943–948.

Joyce, T. M., R. S. Pickart, and R. C. Millard (1999), Long-term hydrographic changes at 52 and 66°W in the North Atlantic subtropical gyre and Caribbean, *Deep Sea Res.*, *46*, 245–278.

Mikolajewicz, U., and R. Voss (2000), The role of the individual air-sea flux components in CO_2-induced changes of the ocean's circulation and climate, *Clim. Dyn.*, *16*, 627–642.

Selten, F. M., G. W. Branstator, H. A. Dijkstra, and M. Kliphuis (2004), Tropical origins for recent and future Northern Hemisphere climate change, *Geophys. Res. Lett.*, *31*, L21205, doi:10.1029/2004GL020739.

Shaffrey, L., and R. Sutton (2004), The interannual variability of energy transports within and over the Atlantic Ocean in a coupled climate model, *J. Clim.*, *17*, 1433–1448.

Shaffrey, L., and R. Sutton (2006), Bjerknes compensation and the decadal variability of the energy transports in a coupled climate model, *J. Clim.*, in press.

Trenberth, K. E., and J. M. Caron (2001), Estimates of meridional atmosphere and ocean heat transports, *J. Clim.*, *14*, 3433–3443.

Wood, R. A., A. B. Keen, J. F. B. Mitchell, and J. M. Gregory (1999), Changing spatial structure of the thermohaline circulation in response to atmospheric CO_2 forcing in a climate model, *Nature*, *399*, 572–575.

Wunsch, C. (2005), The total meridional heat flux and its oceanic and atmospheric partition, *J. Clim.*, *18*, 4374–4380.

S. S. Drijfhout and W. Hazeleger, Royal Netherlands Meteorological Institute (KNMI), P.O. BOX 210, NL-3730 AE, De Bilt, Netherlands. (drijfhou@knmi.nl; hazelege@knmi.nl)